

## **Evaluation of Fiber-Reinforced Asphalt Mixtures Using Advanced Material Characterization Tests**

By

Kamil E. Kaloush, Ph.D., P.E.,  
Associate Professor  
Arizona State University  
Department of Civil and Environmental Engineering  
PO Box 875306, Tempe, AZ 85287-5306  
Telephone: (480)-965-5509  
E-mail: [kaloush@asu.edu](mailto:kaloush@asu.edu)

and

Waleed A. Zeiada  
Krishna P. Biligiri  
Maria C. Rodezno  
Jordan Reed

Graduate Research Associates  
Arizona State University  
Department of Civil and Environmental Engineering  
PO Box 875306, Tempe, AZ 85287-5306  
Telephone: (480)-965-5512  
E-mail:  
[wzeiada@asu.edu](mailto:wzeiada@asu.edu)  
[Krishna.Biligiri@asu.edu](mailto:Krishna.Biligiri@asu.edu)  
[Maria.Rodezno@asu.edu](mailto:Maria.Rodezno@asu.edu)  
[jxreed@asu.edu](mailto:jxreed@asu.edu)

















### E\* Dynamic Modulus Test

The stress-to-strain relationship for an asphalt mixture under a continuous sinusoidal loading is defined by its complex dynamic modulus ( $E^*$ ). In the Mechanistic Empirical Pavement Design Guide (MEPDG), the  $E^*$  Dynamic Modulus of an asphalt mixture is determined per AASHTO TP 62-03. For each mix, three specimens, 4 inches (100 mm) in diameter and 6 inches (150 mm) in height, were tested at 14, 40, 70, 100, and 130 °F and 25, 10, 5, 1, 0.5, and 0.1 Hz loading frequencies. The  $E^*$  tests were done using a controlled sinusoidal stress that produced strains smaller than 150 micro-strain. A master curve was constructed at a reference temperature of 70 °F (21 °C).

Figure 5 (a) shows the average  $E^*$  master curves for both the control and fiber-reinforced asphalt concrete mixtures. The figure can be used for general comparison of the mixtures, but specific comparison of temperature-frequency combination values need to be evaluated separately. That is, one cannot compare direct values on the vertical axis for a specific log reduced time values. As shown in the figure, the fiber-reinforced mixture had higher moduli values than the control mixture at all test temperatures and frequencies. The difference is less at the lowest temperature due to dominant effect of the binder. At higher temperatures, the binder becomes softer and the aggregates dominate the elastic behavior of the asphalt mixtures, and the reinforcement effect of the fibers can enhance the modulus values at higher temperatures. In addition, the aramid fibers have a unique negative thermal coefficient value, in that they contract at higher temperatures and therefore play a positive role in resisting deformation. Figure 5 (b) shows direct comparisons for selected values of test temperatures, 40, 100, and 130 °F (4.4, 37.8 and 54.4 °C) and loading frequency of 10 Hz. It is observed that the modulus values for the fiber-reinforced mixture are higher than the control mixture. Especially at high temperature conditions, the potential rutting field performance of the fiber-reinforced mix would be better than that of the control mixture.

### Fatigue Cracking Test

Load-associated fatigue cracking is one of the major distress types occurring in flexible pavement systems. The action of repeated loading, caused by traffic induced tensile and shear stresses in the bound layers, will eventually lead to a loss in the structural integrity of a stabilized layer material. Fatigue will induce cracks at points where critical tensile strains and stresses occur. The most common model form used to predict the number of load repetitions to fatigue cracking is a function of the tensile strain and mix stiffness (modulus) as follows (6):

$$N_f = K_1 \left( \frac{1}{\epsilon_t} \right)^{k_2} \left( \frac{1}{E} \right)^{k_3} = K_1 (\epsilon_t)^{-k_2} (E)^{-k_3}$$

Where:

$N_f$  = number of repetitions to fatigue cracking

$\epsilon_t$  = tensile strain at the critical location

$E$  = stiffness of the material

$K_1, K_2, K_3$  = laboratory calibration parameters

In this study, beam specimens were prepared for the three point bending test using the reheated mixtures obtained during construction. After compaction to the required density (7% air voids), beams were saw cut to the required dimensions of 2.5 inches (63.5 mm) wide, 2.0 inches

(50.8 mm) high, and 15 inches (381 mm) long. A full testing factorial was used for each mixture: constant strain, 6 to 8 levels, and one replicate for each test temperature. Three temperature levels, 40, 70, 100 °F, (4.4, 21, and 38.8 °C) were used. Initial flexural stiffness was measured at the 50<sup>th</sup> load cycle. Fatigue life or failure under control strain was defined as the number of cycles corresponding to a 50% reduction in the initial stiffness as required by AASHTO TP8 and SHRP M-009.

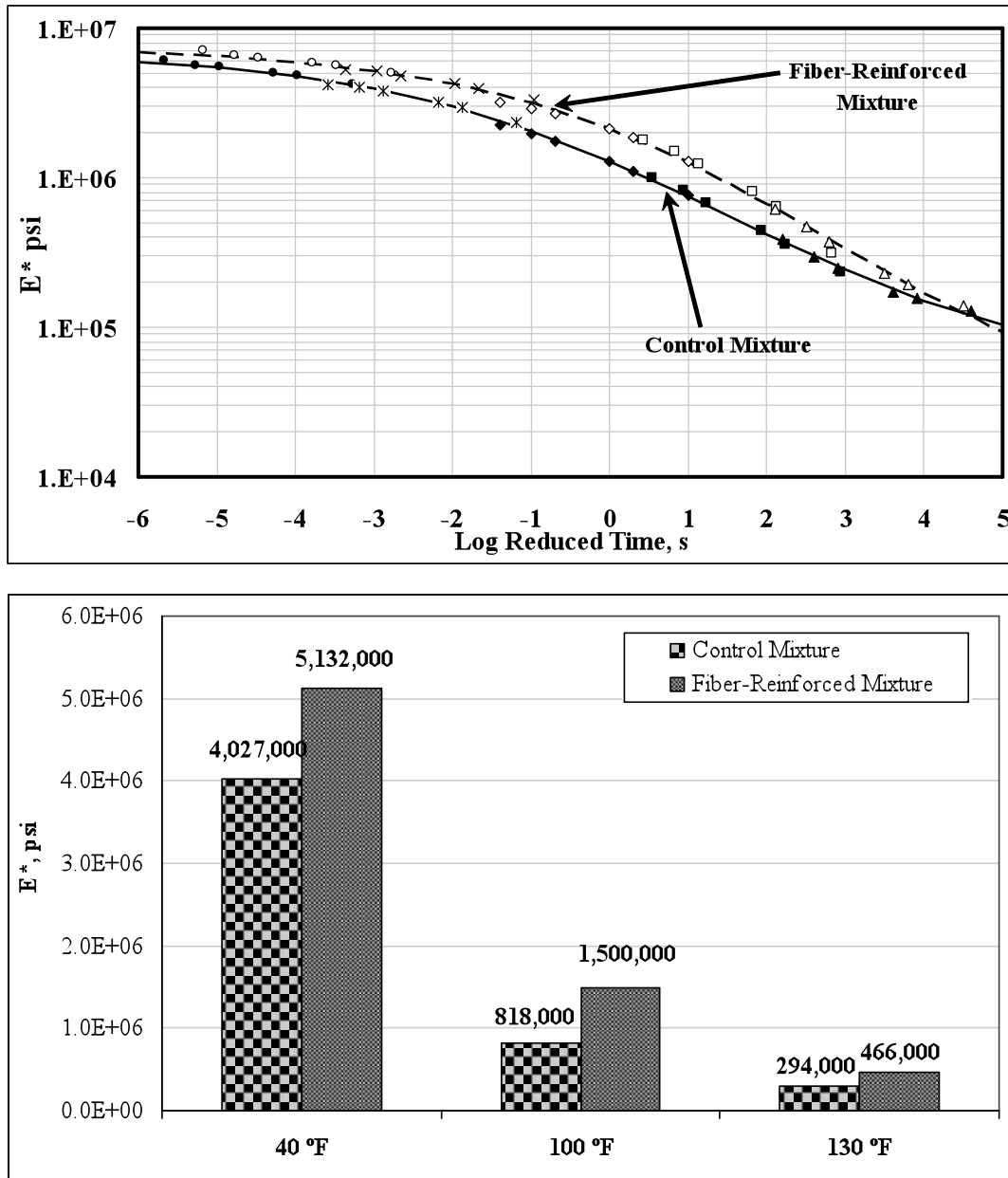


**FIGURE 5 (a) Unconfined Dynamic Modulus Master Curves; (b) Comparison of Measured Dynamic Modulus Values at 10 Hz.**

Fatigue relationships for both mixtures were developed. The regression equations for each temperature ( $N_f = K_1 \cdot \epsilon^{K_2}$ ) were also computed along with the coefficient of determination

( $R^2$ ) for each relationship. Figure 6 shows a comparison of fatigue relationships for the control and fiber-reinforced asphalt concrete mixtures at 70 °F. It is observed that the fatigue life is higher for the control mixture at high strain values while the fiber-reinforced mixture has higher fatigue life at lower strain values.

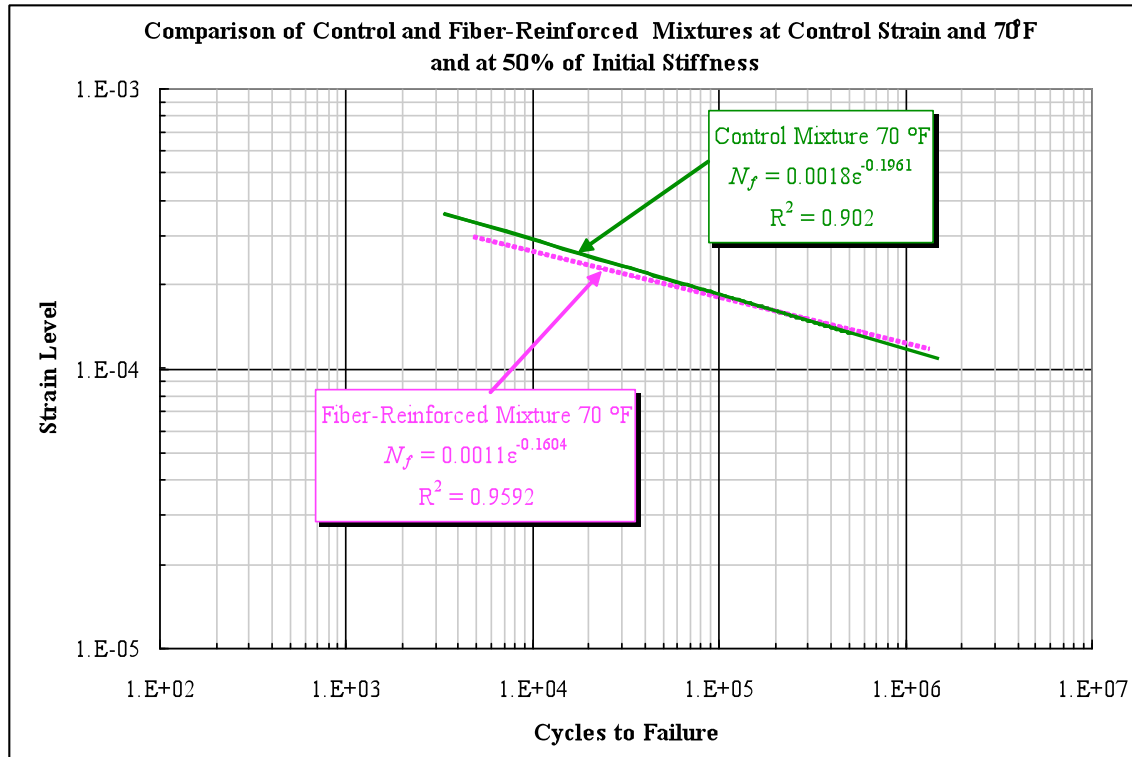


**FIGURE 6 Comparison of Fatigue Relationships for both Mixtures at 70 °F.**

Table 3 summarizes the  $K_1$ ,  $K_2$ , and  $K_3$  Coefficients of the generalized fatigue model for both mixtures (at 50% reduction of the initial stiffness). The initial stiffness was measured at  $N = 50$  cycles. These generalized fatigue relationships show excellent measures of accuracy for both mixtures.

**TABLE 3 Summary of the Regression Coefficients for the Generalized Fatigue Equation**

Mixture Type	50% of Initial Stiffness, $E_o$ @ $N=50$ Cycles			
	$K_1$	$K_2$	$K_3$	$R^2$
Control	2.3496	2.3601	1.3853	0.914
Fiber-Reinforced	6.48E-22	7.8357	1.0839	0.988

$$* N_f = K_1 * (1/\epsilon_t)^{K_2} * (1/E_o)^{K_3}$$

An example comparing the fatigue life for both mixtures was predicted using the regression coefficients  $K_1$ ,  $K_2$ , and  $K_3$  at 70 °F and two different strain levels. The results are

shown in Figure 7. At 150 micro-strains level, the fiber-reinforced mixture shows approximately 2 times higher fatigue life compared to the control mixture; while at 200 micro-strains level, the control mixture shows approximately 3 times higher fatigue life compared to the fiber-reinforced mixture. The shift in predicted fatigue life suggests that the fiber-reinforced mix will perform better in roads where traffic speeds are higher. This type of fatigue testing is a disadvantage for a stiffer material like the fiber-reinforced mixture. These results may be labeled as inconclusive, and is worthy of more investigation.

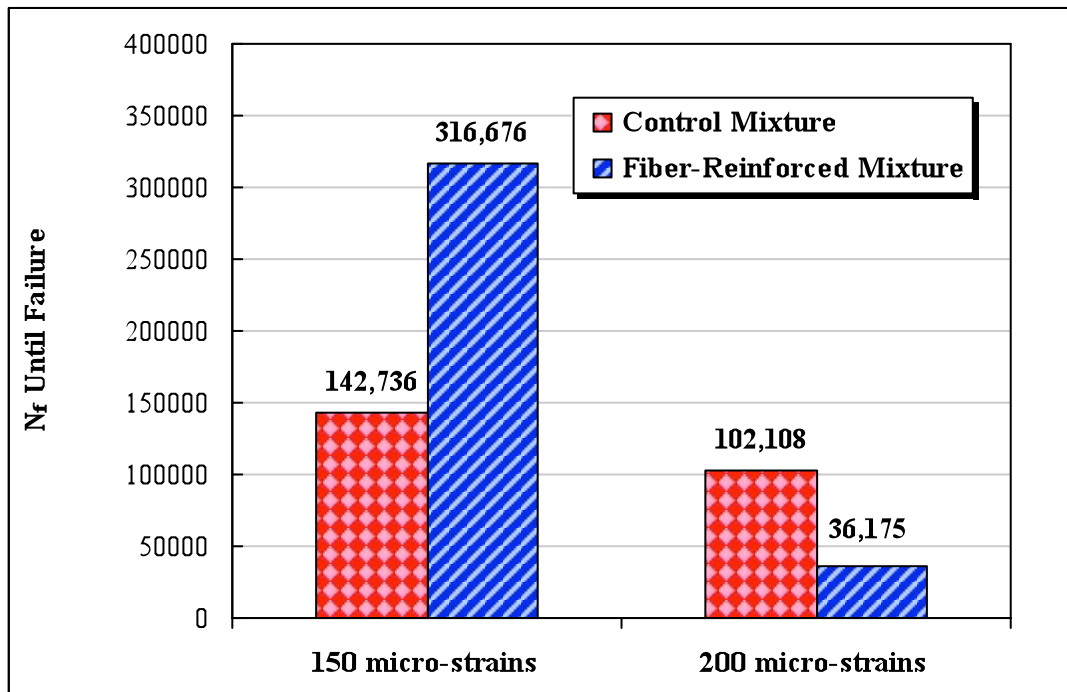


**FIGURE 7** Number of Cycles to Failure Predicted for Both Mixtures at 150 and 200 micro-strains and at 70 °F.

### Thermal Cracking Test

Standard test method for determining the creep compliance and strength of HMA using the indirect tensile test device per AASHTO TP9-02 was utilized to evaluate low temperature thermal cracking performance of the control and the fiber-reinforced asphalt concrete mixtures (7, 8). Figure 8 presents the tensile strength test results for both mixtures. The fiber-reinforced asphalt mixture has 1.5 times higher strength than the control mixture. Higher thermal cracking would be expected for mixtures with lower tensile strength values (4). In essence, the fibers in the mix are believed to play a vital role in resisting thermal cracking in the HMA mixture.

The consideration of the total fracture energy is another useful comparison from this test. The results are shown in Figure 9. The fracture energy increased with increasing temperature for both the mixtures. At all test temperatures, the fiber-reinforced asphalt mixture had consistently higher fracture energy than the control mix. Generally, lower thermal cracking should be expected as the fracture energy is increased (4).

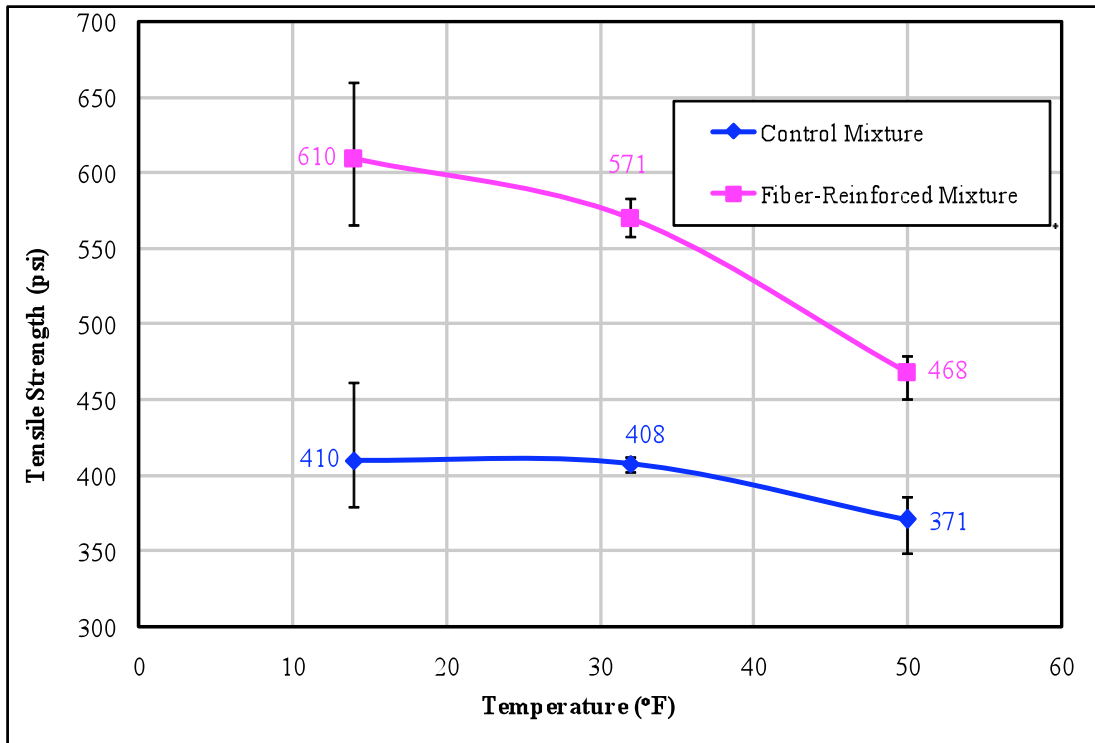


**FIGURE 8 Comparison of the Tensile Strength Results.**

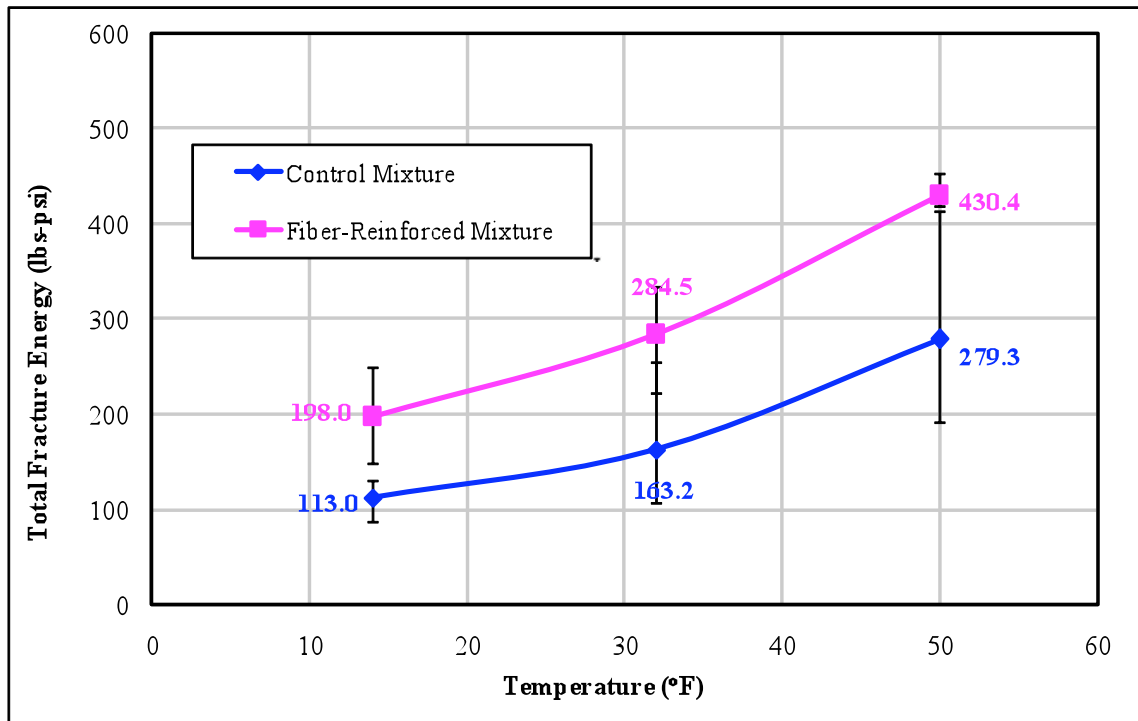


**FIGURE 9 Comparison of the Total Fracture Energy Results.**

### Crack Propagation - C\* Line Integral Test

Fracture mechanics provides the underlying principles which govern initiation and propagation of cracks in materials. Sharp internal or surface notches which exist in various materials intensify local stress distribution. If the energy stored at the vicinity of the notch is equal to the energy required for the formation of new surfaces, then crack growth can take place. Material at the vicinity of the crack relaxes, the strain energy is consumed as surface energy, and the crack grows by an infinitesimal amount. If the rate of release of strain energy is equal to the fracture toughness, then the crack growth takes place under steady state conditions and the failure is unavoidable (9).

The concept of fracture mechanics was introduced to asphalt concrete by Majidzadeh (10). Abdulshafi applied the energy (C\*-Line Integral) approach to predicting the pavement fatigue life using the crack initiation, crack propagation, and failure (11). Abdulshafi, O., and Abdulshafi, A. and Kaloush used notched disk specimens to apply J-integral concept to the fracture and fatigue of asphalt pavements (11, 12).

#### C\* Parameters

The relation between the J-integral and the C\* parameters is a method for measuring it experimentally. J is an energy rate and C\* is an energy rate or power integral. An energy rate interpretation of J has been discussed by Rice; and Begley and Landes (13, 14). J can be interpreted as the energy difference between the two identically loaded bodies having incrementally differing crack lengths.

$$J = - \frac{dU}{da}$$

Where,

U = Potential Energy

a = Crack Length

C\* can be calculated in a similar manner using a power rate interpretation. Using this approach C\* is the power difference between two identically loaded buddies having incrementally differing crack lengths.

$$C^* = - \frac{\partial U^*}{\partial a}$$

Where U\* is the power or energy rate defined for a load p and displacement u by:

$$U^* = \int_0^u p du$$

#### Method for C\* Determination

Disc samples were prepared from gyratory plugs similar to the IDT specimen preparation process. For each disc, a right-angle wedge was cut into the specimen to accommodate the loading device as shown in Figure 10. Tests were conducted at 21° C.

The load applied at a constant displacement rate and the crack length over time were measured for each test specimen. The displacement rates used were 0.005, 0.01, 0.015, 0.02, and 0.025 in/min for both the control and fiber-reinforced mixtures. The data was used to determine load as a function of displacement rate for various crack lengths. The power of energy rate input, U\*, was measured as the area under the load displacement rate curve. The energy rate, U\*, was

then plotted versus crack length for different displacement rates and the slopes of these curves constituted the C\*-integral. The C\*-integral was plotted as a function of the displacement rate. Finally, the C\* integral data were plotted as a function of the crack growth rate as shown in Figure 11. In this figure, it is observed that the fiber-reinforced mixture has much higher C\*-integral and slope values compared to the control mixture. This is an indication that the fiber-reinforced mixture has much higher resistance to crack propagation. A unique observation of the fiber-reinforced mix specimens after the test was that the samples never split and they were difficult to split them apart by hand; whereas most of the control mixture samples split at the end of the test.

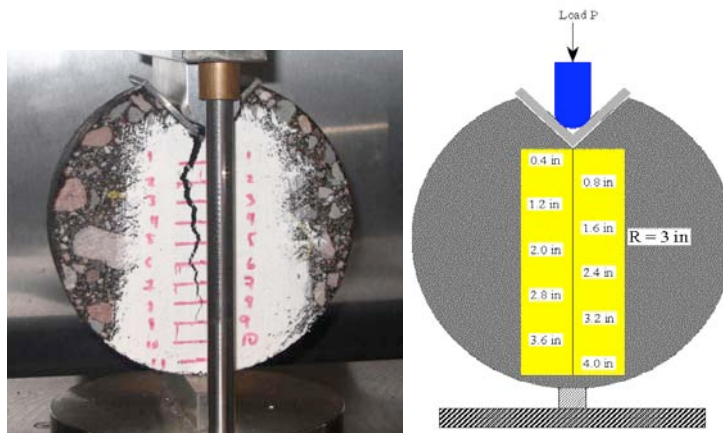


FIGURE 10 Typical C\* Test Setup.

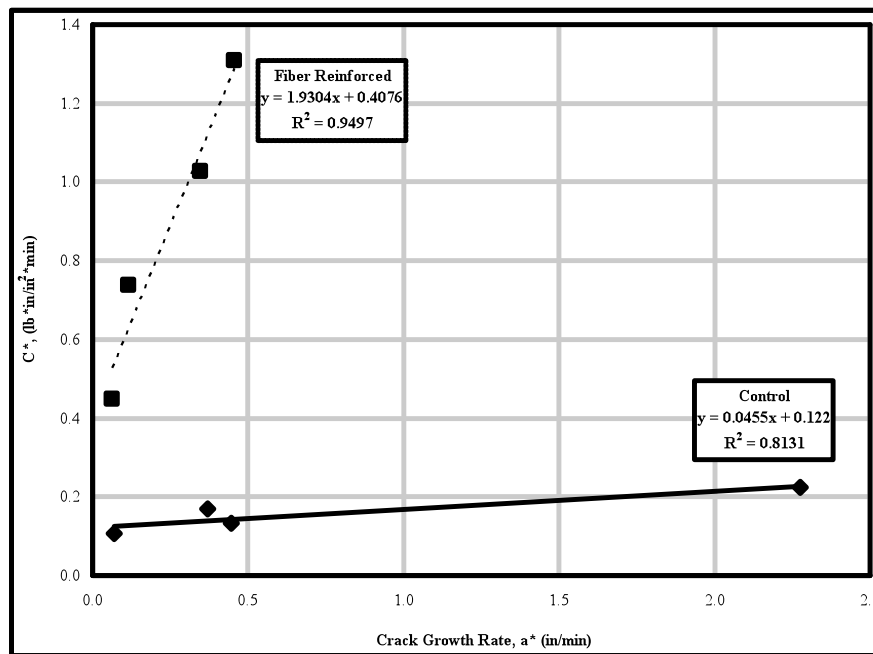


FIGURE 11 C\* Line Integral versus Crack Growth Rate.

## CONCLUSIONS

A mixture of polypropylene and aramid fibers was used in a field and laboratory study to evaluate the performance characteristics of the modified asphalt mixture. The laboratory experimental program on the field mixes included: triaxial shear strength, dynamic (complex) modulus, repeated load permanent deformation, beam fatigue, crack propagation, and indirect diametral tensile tests. The data was used to compare the performance of the fiber modified mixture to the control. The results showed that the fibers improved the mixture's performance in several unique ways as summarized below:

- The fiber-reinforced asphalt mixture showed better resistance to shear deformation as shown by the triaxial shear strength test results. Notably, post peak failure for the fiber-reinforced asphalt mixture showed higher residual energy and gradual drop in strength, an effect that was attributed to the influence of the fibers in the mix.
- Permanent deformation tests for the fiber-reinforced mixture showed lower permanent strain accumulation compared to the control mix. The flow number results, or the beginning of tertiary stage, were 15 times higher than the control mixture. Two characteristics were observed for the fiber-reinforced mixture in these tests: an extended endurance period in the secondary stage of the permanent deformation curve, and the gradual (less) accumulation of permanent strain beyond tertiary flow. Both of these characteristics were attributed to the presence and mobilization of the fibers distributed in the mix.
- The measured Dynamic Modulus  $E^*$  values were higher for the fiber-reinforced mix. The difference between the two mixtures was less at the lowest temperature (20% increase), due to dominant effect of the binder and less contribution of the role of fibers. The largest difference was observed at 100°F (80% higher), where the reinforcement effect of the fibers is observed to be the highest. At 130°F, the increase in modulus was also substantial at about 50%.
- The fatigue cracking test was different in that, unlike the other tests, the strain level was held constant. The fatigue life was higher for the control mixture at high strain values while the fiber-reinforced mixture had higher fatigue life at lower strain values. The shift in predicted fatigue life suggests that the fiber-reinforced mix will perform better in roads where traffic speeds are higher. However, it was concluded that the fatigue cracking results are inconclusive and need further evaluation.
- The tensile strength and fracture energy measured from the IDT test showed that at all test temperatures, the fiber-reinforced mix exhibited the highest values; an increase of 25 to 50% for the tensile strength, and 50 to 75% for the fracture energy. Generally, lower thermal cracking should be expected as the tensile strength and fracture energy are increased.
- Relationships between crack growth rates and  $C^*$  line integral values showed that the fiber-reinforced mix had about 40 times higher resistance to crack propagation than the control mix.
- A field condition survey after approximately one year (with two summer periods included) revealed that there are a couple of low severity cracks, 1 to 2 feet long, in the control section. No cracks were observed in the fiber-reinforced pavement sections.



## ACKNOWLEDGEMENTS

The authors would like to acknowledge FORTA Corporation for providing the fibers. Acknowledgements are also due to CEMEX (formally Rinker West, Central Region) for their assistance in the production and construction of the test section. City of Tempe engineering department and personnel for their invaluable assistance in providing the field test section at Evergreen Drive and for their help in coordinating the construction activities. Special thanks are also due to Mr. Kenny Witczak, Supervisor of the Advanced Pavement Laboratory at ASU for the production and preparation of the laboratory test specimens.

## REFERENCES

1. Bueno, B. S., Silva, W. R., Lima, D. C., Minete, E. (2003). Engineering Properties of Fiber Reinforced Cold Asphalt Mixes. Technical Note, *Journal of Environmental Engineering*, ASCE, Vol. 129, N. 10.
2. FORTA Corporation (2005), U.S.A. Report #30-02, Grove City, Pennsylvania, USA.
3. Lee, S. J., Rust, J. P., Hamouda, H., Kim, Y. R., Borden, R. H. (2005). Fatigue Cracking Resistance of Fiber-Reinforced Asphalt Concrete. *Textile Research Journal*, Vol. 75, N. 2, pp. 123-128.
4. Witczak, M. W., Kaloush, K. E., Pellinen, T., El-Basyouny, M., & Von Quintus, H. (2002). Simple Performance Test for Superpave Mix Design. *NCHRP Report 465*. Transportation Research Board. National Research Council. Washington D.C.
5. Witczak, M. W. and M. W. Mizra. (1995). Development of Global Aging System for Short and Long Term of Asphalt Cements. *Journal of the Association of the Asphalt Paving Technologists*, Vol. 64, pp.532-572
6. SHRP-A-404. Fatigue Response of Asphalt-Aggregate Mixes. Asphalt Research Program, Institute Of Transportation Studies, University Of California, Berkeley. Strategic Highway Research Program, National Research Council, Washington, D.C., 1994.
7. Witczak, M.W., "Harmonized Test Methods for Laboratory Determination of Resilient Modulus for Flexible Pavement Design, Volume II - Asphalt Concrete Material", Final Project Report, NCHRP Project No. 1-28A, May 2003.
8. Roque et al, "Standard Test Method for Determining the Creep Compliance and Strength of Hot Mix Asphalt (HMA) Using the Indirect Tensile Test Device", Draft Test Protocol, AASHTO TP9-02, 2002.
9. Mamlouk, M. S. and Mobasher, B. (2004). "Cracking Resistance of Asphalt Rubber Mix versus Hot-Mix Asphalt", *International Journal of Road Materials and Pavement Design*. V.5., 4, pp. 435-452.
10. Majidzadeh, K. (1976). "Application of Fracture Mechanics for Improved Design of Bituminous Concrete," Volumes 1 and 2, Report FHWA-RD-76-91, Federal Highway Administration, Washington, D.C.

11. Abdulshafi, O., (1983). "Rational Material Characterization of Asphaltic Concrete Pavements," Ph.D. Dissertation, the Ohio State University, Columbus, OH, 1983.
12. Abdulshafi, A. and K.E. Kaloush. "Modifiers for Asphalt Concrete." ESL-TR-88-29, Air Force Engineering and Services Center, Tyndall Air Force Base, Florida, 1988.
13. Rice. J. R., (1968). Journal of Applied Mechanics, American Society of Mechanical Engineers, Volume 35, pp. 379-386.
14. Begley, J. W. and Landes, J. D., (1972). Fracture Toughness, Processing of the 1971 National Symposium on Fracture Mechanics. Part II, ASTM STP 514, American Society for Testing Materials pp. 1-20.